

# Monofluorinated Nitrogen Containing Heterocycles: Synthesis, Characterization and Fluorine Effect

Marco Reichel<sup>[a]</sup> and Konstantin Karaghiosoff<sup>\*[a]</sup>

*Dedicated to Professor Dr. Herbert W. Roesky on the occasion of his 85th birthday*

**Abstract.** A straight forward synthesis and efficient introduction of fluoromethyl group in nitrogen heterocycles is reported. Starting from the respective NH heterocycles fluoromethylation is performed with fluoroiodomethane and proceeds under mild reaction conditions. Structural information of monofluoromethylated nitrogen-containing cyclic

compounds containing the biologically active NCH<sub>2</sub>F moiety are reported. The particularly impressively change of physical and spectroscopic properties by the substitution of a methyl group by a monofluoromethyl group is discussed based on these examples.

## Introduction

Nitrogen containing heterocycles with a fluoromethyl group directly bonded to nitrogen are of great interest due to their application in different areas. While heterocycles with the NCH<sub>2</sub>F structural motive have been used as reagents in nickel catalyzed cross coupling reactions,<sup>[1]</sup> most of their applications are related to biologically active compounds. Five membered nitrogen heterocycles with an N-bonded CH<sub>2</sub>F group are used for agro chemicals, especially for microbiocides and herbicides.<sup>[2]</sup> In addition, based on the bioisosteric relationship between CH<sub>2</sub>F and a variety of functional groups, they are essential for the pharmaceutical industry. Thus, NCH<sub>2</sub>F containing heterocycles act as biologically active building blocks in endothelial lipase inhibitors (**1**),<sup>[3]</sup> in agents for the treatment of CRF-1 related disorders (**2**)<sup>[4]</sup> or acting as choline transporter inhibitors (**3**) (Figure 1).<sup>[5]</sup>

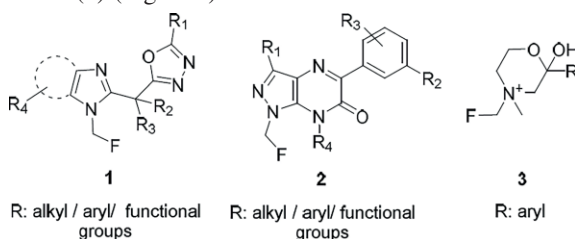


**Figure 1.** Biological active NCH<sub>2</sub>F containing heterocycles.

\* Prof. Dr. K. Karaghiosoff  
E-Mail: [klk@cup.uni-muenchen.de](mailto:klk@cup.uni-muenchen.de)

[a] Department of Chemistry  
Ludwig-Maximilian-University  
Butenandtstr. 5–13 (D)  
81377 Munich, Germany

Supporting information for this article is available on the WWW under <http://dx.doi.org/10.1002/zaac.202000239> or from the author.

© 2020 The Authors. Published by Wiley-VCH Verlag GmbH & Co. KGaA. • This is an open access article under the terms of the Creative Commons Attribution License, which permits use, distribution and reproduction in any medium, provided the original work is properly cited.

Due to the strong and polar C–F bond the introduction of fluorine in organic compounds changes (in part dramatically) their physical properties and compounds with unique physical and properties can be obtained.<sup>[6]</sup> Monofluoromethyl diaalkylamines are a good example; unlike the corresponding chloro-, bromo- and iodomethyl analogues they no longer have a salt-like character.<sup>[7]</sup> This affects the boiling / melting points as well as the solubility and reaction behavior. The synthesis of amines with a fluoromethyl group attached to nitrogen is still a challenge, however. It is well known, that fluoromethyl halides CH<sub>2</sub>FCl, CH<sub>2</sub>FBr and CH<sub>2</sub>FI can be used for electrophilic fluoromethylation of various oxygen-, sulfur-, carbon- and nitrogen- nucleophiles.<sup>[8]</sup> While secondary fluoromethylamines are likely to eliminate hydrogen fluoride and are of limited stability, tertiary fluoromethylamines and N–CH<sub>2</sub>F ammonium salts are stable and are prepared starting from the corresponding secondary or tertiary amines by reaction mostly with CH<sub>2</sub>FCl.<sup>[8,9]</sup> However, the use of cheap CH<sub>2</sub>FCl and CH<sub>2</sub>FBr as fluoromethylating agents becomes increasingly problematic due to the ozone depleting properties of these compounds. In addition, handling of volatile CH<sub>2</sub>FCl and CH<sub>2</sub>FBr is challenging, particularly taking into account the harsh reaction conditions necessary.<sup>[6,8]</sup>

Structural information is of crucial importance in development and design of new pharmaceutically active agents. Although a large number of nitrogen compounds with a N-bonded CH<sub>2</sub>F group have been prepared and many of them are used as pharmaceutical drugs, surprisingly practically no structural information is available for the NCH<sub>2</sub>F motive. Only one crystal structure – that of Me<sub>3</sub>NCH<sub>2</sub>F<sup>+</sup> PbI<sub>3</sub><sup>–[10]</sup> – has been described in the literature so far.

Herein, we report a simple and practical method to synthesize new monofluoromethylated nitrogen heterocycles under mild reaction conditions with high yields using fluoroiodomethane. The change in physical properties and the influence of fluorine were investigated by comparing the CH<sub>2</sub>F containing new nitrogen heterocycles with the corresponding methyl or

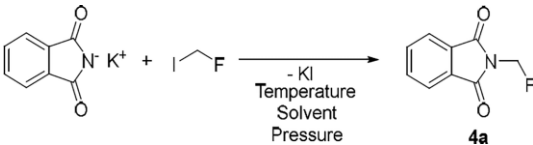
hydroxymethyl derivatives. The molecular and crystal structures of selected nitrogen heterocycles containing the NCH<sub>2</sub>F group were determined by single-crystal X-ray diffraction and offer an insight on the structural properties of this fascinating building block.

## Results and Discussion

*N*-Fluoromethyl phthalimide (**4**) is an important intermediate in the production of agrochemicals acting as herbicides or microbiocides.<sup>[11]</sup> Its synthesis starting from phthalimide and introducing the CH<sub>2</sub>F group by reaction with CH<sub>2</sub>FCl is unattractive due to the low yield (23%), while alternative routes are more complicated and more expensive.<sup>[12]</sup> Parallel to our investigation *Pace et al.* reported, that compound **4a** can be obtained in a high (82%) starting from the Cs salt of phthalimide using fluoroiodomethane.<sup>[12c]</sup>

For the synthesis of **4** we have used potassium phthalimide as the starting material, which was readily prepared from phthalimide according to a modified literature known procedure.<sup>[14]</sup> Reaction of potassium phthalimide with CH<sub>2</sub>FI results in the formation of **4**, which can be readily isolated by crystallization. The reaction conditions were optimized to give the best yield of 71% (Table 1).

**Table 1.** Optimization of the reaction conditions for the synthesis of **4**.



Entry	<i>T</i> / °C	<i>p</i> / bar	Solvent	<i>t</i> / h	Yield / %
1	35.6	1	Et <sub>2</sub> O	3	5
2	40	1	DCM	3	12
3	82	1	CH <sub>3</sub> CN	3	34
4	100	7	Et <sub>2</sub> O	3	9
5	100	6.1	DCM	3	39
6	100	1,9	CH <sub>3</sub> CN	3	52
7	120	3,3	CH <sub>3</sub> CN	3	71

Potassium phthalimide was refluxed at ambient pressure in different solvents. The resulting yields were nearly as poor as for CH<sub>2</sub>FCl (23%), the reaction in acetonitrile giving the best results (Table 1). In a previous study it was shown that fluoromethylation under increased pressure can lead to better yields.<sup>[6,13]</sup> Following this experience we performed the synthesis in a pressure tube and in fact for all solvents the yields of **4** were higher at 100 °C as compared to ambient conditions (Table 1). This further confirms the great impact of the pressure for fluoromethylation reactions with CH<sub>2</sub>FI. Acetonitrile as solvent led to the highest yield (52%). The yield could be further improved to 71% by performing the reaction in acetonitrile at 120 °C. Higher temperatures resulted in a brownish color of the reaction solution most probably indicating decomposition. Single crystals of compound **4** were obtained by slow evaporation of the acetonitrile solution. Unexpectedly single

crystals of the corresponding hydroxymethyl derivative **5** formed in the crystallization batch after one month at ambient temperature, most probably due to slow hydrolysis of the NCH<sub>2</sub>F group. A similar behavior has been observed in the case of primary fluoromethylamines.<sup>[8]</sup> The molecular structures of **4** and **5** in the crystal are shown in Figure 2.

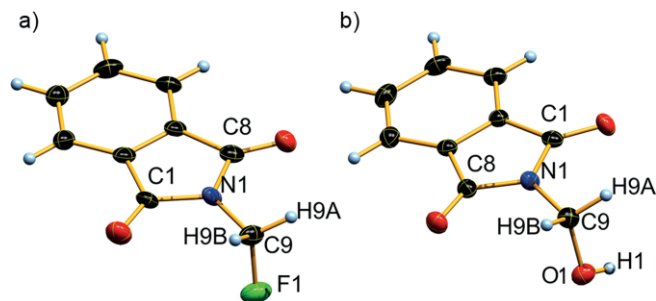


**Figure 2.** Molecular structure of **4** (a) and **5** (b) in the crystal. DIAMOND representation, thermal ellipsoids are shown with 50% probability. Selected bond length and angles of **4**: N1–C9, 1.427(4); C9–F1, 1.388(3); F1–C9–N1, 109.3(2); F1–C9–N1–C1, 95.6(3).

The crystal structures of **4** and **5** offer the unique possibility to compare the structural behavior of two molecules differing only in F / OH at the same position. In both cases the molecules are completely planar and only the functional groups (F and OH) are positioned out of the molecular plane. The most interesting feature of the molecular structure of **4** is the NCH<sub>2</sub>F group. The nitrogen atom in **4** and **5** displays a trigonal planar environment. The N1–C9 distance of 1.427(4) Å in **4** is somewhat shorter as compared to the N1–C9 distance of 1.456(3) Å in **5** and significantly shorter as compared to the distance of 1.51(2) Å reported for the Me<sub>3</sub>NCH<sub>2</sub>F cation.<sup>[10]</sup> In this last case, however, the CH<sub>2</sub>F group is disordered and structural parameters are less accurate. The C9–F1 bond length [1.388(3) Å] compares well to the value of a 1.399 Å for a C<sub>sp</sub><sup>3</sup>–F single bond, found in the literature<sup>[14]</sup> and also to the C,F distance reported for the PCH<sub>2</sub>F group [1.379(5) Å] (Figure 2).<sup>[6]</sup> However, the CH<sub>2</sub>–F bond length is shorter than the C,O distance in the bioisosteric CH<sub>2</sub>–OH moiety in **5** of 1.402(3) Å and the Me<sub>3</sub>NCH<sub>2</sub>F cation with 1.43(2) Å.<sup>[10]</sup> There are considerable differences in the physical properties between **4** and **5**. For example, with a melting point of 82 °C, **4** is melting much lower than **5** (168 °C)<sup>[15]</sup> or the analogous methyl derivative (CH<sub>3</sub> in place of CH<sub>2</sub>F, 134 °C).<sup>[16]</sup> In order to understand the difference in physical properties of the fluoromethyl compound **4** and the hydroxymethyl compound **5** it is necessary to look into the interactions in the crystal (Figure 3).

In the case of **5** the OH group acts as H-donor and undergoes hydrogen bonding with the oxygen atom of one of the carbonyl groups. This results in the formation of chains of hydrogen bonded molecules of **5** in the crystal. In the case of **4** the electronegative fluorine atom can act only as a H-acceptor in hydrogen bonding and interactions are less strong as compared to **5**. The strongest interactions are between a proton of CH<sub>2</sub> and the oxygen atom of C=O of another molecule, followed by the interaction between fluorine of the same CH<sub>2</sub>F group and an aromatic proton of the same second molecule.

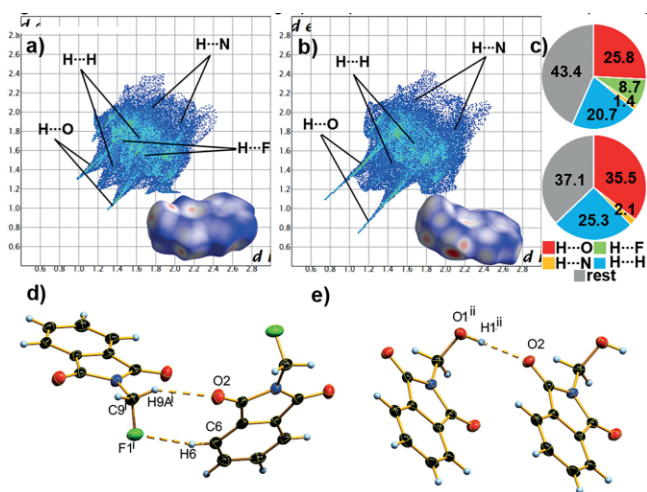
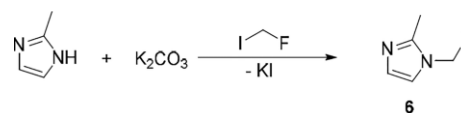


**Figure 3.** Two-dimensional fingerprint plot as well as the corresponding Hirshfeld surface (bottom right in 2D plot) of **4** (a) and **5** (b). Color coding: white, distance  $d$  equals VDW distance; blue,  $d$  exceeds VDW distance; red,  $d$  is smaller than VDW distance. Population of close contacts of **4** (top) and **5** (bottom) in crystal stacking. View of hydrogen bonding in **4** (d) and **5** (e), showing the strongest interactions. DIAMOND representation. Thermal ellipsoids are drawn at 50% probability level. Symmetry code:  $i$ )  $1-x, 0.5+y, -z$ ;  $ii$ )  $1+x, y, z$ .

This also results in the formation of chains in the crystal of **4** with the only difference of weaker interactions. This behavior is confirmed also by the Hirshfeld analysis of the structures of **4** and **5**. For strong O–H bonding the 2D fingerprint plot exhibits two distinct spikes.<sup>[17]</sup> Comparing Figure 2a and b it becomes obvious, that O–H hydrogen bonding in **5** is much stronger than in **4**. Evaluation of the population of the close contacts (Figure 3c) shows, that **5** with 35.5% O...H close contacts displays more H-bridges than **4**. With respect to  $d_i + d_e$  ( $d_i$ : distance from the Hirshfeld surface to the nearest atom interior;  $d_e$ : distance from the Hirshfeld surface to the nearest atom exterior) we can follow that 8.7% F...H contacts for **4** are weak due to their long distance and so these interactions cannot compensate the lower number of O...H contacts in **4**. The hydrogen bonding in Figure 3d and 3e shows the shortest contacts in the crystal. Considering these short contacts as well as the angles at the respective hydrogen atoms of  $175(3)^\circ$  in

**5** and of  $150(1)^\circ, 163(2)^\circ$  in **4** (Table 2), the intermolecular interactions in **5** are considered to be stronger than in **4**.<sup>[18]</sup> This is in accord with and explains the dramatic difference of the melting points of both compounds.

Another pair of heterocycles, which can be compared and display the effect of fluorine are 1*H*-2-methylimidazole<sup>[19]</sup> and the new 1*H*-1-fluoromethyl-2-methylimidazole **6**. Similar to the synthesis of **4**, the fluoromethyl derivative **6** was obtained by reaction of potassium 2-methylimidazolite with  $\text{CH}_2\text{FI}$  (Scheme 1). However, parallel to this publication, Pace et al. reported that imidazole and other nitrogen containing heterocycles can also be *N*-fluoromethylated in high yields starting from the corresponding Cs with fluoroiodomethane.<sup>[12c]</sup> Potassium 2-methylimidazolite is readily prepared starting from 1*H*-2-methylimidazole by reaction with potassium carbonate.<sup>[20]</sup> Fluoromethyl imidazole **6** is isolated as a slightly yellowish oil (63% yield), which tends to form a super cooled melt.



**Scheme 1.** Synthesis of fluoromethyl imidazole **6**.

Single crystals of **6a** and its monohydrate **6b** (Figure 4) were formed by slow evaporation of a solution of **6** in chloroform. The nitrogen atom in **6a** and **6b** displays a trigonal planar environment, as observed for **4** (Figure 2). The N2–C5 distance to the fluoromethyl group in both, **6a** [1.420(3) Å] and the hydrate **6b** [1.423(2) Å] is almost the same and in good agreement with that found in **4** [1.427(4) Å]. The crystal water seems to not affect the C5–F1 bond length. With values of 1.400(3) Å (**5**) and 1.388(2) Å (**6b**) these distances fit well to that observed in the case of **4** [1.388(3) Å]. However, somewhat shorter C,F distances are reported for  $\text{PCH}_2\text{F}$  [1.379(5) Å],<sup>[6]</sup>  $\text{CH}_2\text{FI}$  [1.380(17) Å],<sup>[21]</sup> and  $\text{CH}_2\text{FBr}$  [1.377(4) Å].<sup>[21]</sup> Compounds **6a** and **6b** mainly differ in the intermolecular interactions in the crystal (Figure 3).

**Table 2.** Bond length /Å and bond angles /° of selected hydrogen bonds.

Compound	Bond	$d(D-H)$	$d(H\cdots A)$	$d(D\cdots A)$	$D-H\cdots A$
<b>4</b>	C9 <sup>i</sup> –H9A <sup>i</sup> ...O2	0.96(2)	2.416(2)	3.284(4)	150(1)
	C6–H6...F1 <sup>i</sup>	0.99(4)	2.68(3)	3.651(5)	163(2)
<b>5</b>	O1 <sup>ii</sup> –H1 <sup>ii</sup> ...O2	0.86(3)	1.98(4)	2.835(3)	175(3)
<b>6a</b>	C4–H4B...F1 <sup>i</sup>	0.98	2.593(2)	3.420(3)	142(2)
<b>6b</b>	C2–H2...O1	0.96(2)	2.39(2)	3.329(2)	166(2)
	O1–H3...N1 <sup>ii</sup>	0.83(2)	1.97(2)	2.795(2)	174(2)
	C1 <sup>ii</sup> –H1 <sup>ii</sup> ...F1	0.95	2.686(2)	3.563(2)	153.81(8)
<b>7</b>	C4–H4A...F1 <sup>i</sup>	0.91(2)	2.49(2)	3.221(3)	137(2)
	C6–H6B...F2 <sup>iii</sup>	0.92(2)	2.37(2)	3.055(3)	131.0(8)
	C6–H6A...I1	0.92(2)	3.59(2)	4.005(3)	110.4(8)
	C1 <sup>iii</sup> –H1 <sup>iii</sup> ...I1	0.90(3)	3.16(3)	3.954(3)	148(2)
	C6 <sup>iii</sup> –H6B <sup>iii</sup> ...I1	0.92(2)	3.49(2)	4.159(3)	131.8(7)

Symmetry code: **4**)  $i$ )  $1-x, 0.5+y, -z$ ; **5**)  $ii$ )  $1+x, y, z$ ; **6a**)  $i$ )  $0.5+x, 0.5-y, 1-z$ ; **6b**)  $i$ )  $0.5+x, 0.5-y, 1-z$ ;  $ii$ )  $1-x, -0.5+y, 0.5-z$  **7**)  $i$ )  $1-x, -y, -z$ ;  $iii$ )  $1.5-x, 0.5+y, z$ .



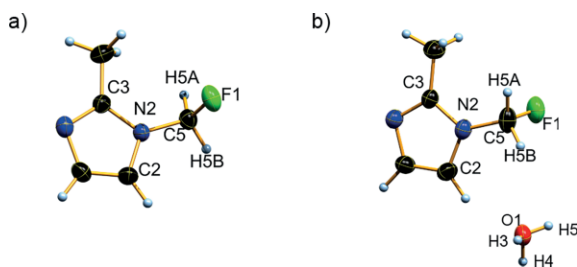
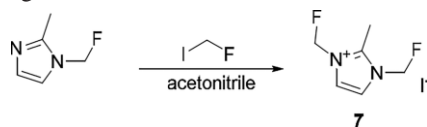


**Figure 4.** Molecular structure of **6a** (a) and of the monohydrate **6b** (b) in the crystal. In the case of **6b** one proton of the H<sub>2</sub>O molecule is disordered over two positions (50% disorder). DIAMOND representation, thermal ellipsoids are drawn with 50% probability. Selected bond length and angles of **6a**: C5–F1, 1.400(3); C5–N2, 1.420(3); N2–C5–F1, 109.3(2); F1–C5–N2–C3, –84.3(3). **6b**: C5–F1, 1.388(2); C5–N2, 1.423(2); F1–C5–N2, 109.8(2); F1–C5–N2–C3, –84.8(2).

Looking at the Hirshfeld analysis of the structures of **6a** and **6b**, from the distinct spikes in the 2D Plot it becomes evident, that the H $\cdots$ F interactions in the sum are less but stronger,<sup>[17]</sup> as compared to **6a** (Figure 6a–c). The larger angle at hydrogen of 166(2) $^\circ$  in **6b** as compared to 142(2) $^\circ$  in **6a** (Table 2) confirms that intermolecular H $\cdots$ F interactions in **6b** are stronger than in **6a** (Figure 6f, g).<sup>[18]</sup> The sum  $d_i + d_e$  ( $d_i$  = distance from the Hirshfeld surface to the nearest atom interior;  $d_e$  = distance from the Hirshfeld surface to the nearest atom exterior) indicates, that for **6a** in general all interactions in the crystal are very weak (Table 2), due to the long distances of the H $\cdots$ N and H $\cdots$ F contacts (Figure 6a) and the angles at hydrogen with values of 142(2)–175(2) $^\circ$ .<sup>[17–18]</sup> The low melting point of 27  $^\circ$ C observed for **6a** is in accord with these weak interactions. Compared to its methyl analogue (m.p. 51  $^\circ$ C; b.p. 206  $^\circ$ C),<sup>[22]</sup> **6a** shows lower melting and boiling points. This is in good agreement with the observation made for **4**, where the melting point of which is about 50  $^\circ$ C lower than that of the corresponding methyl derivative.

Fluoromethyl imidazole **6a** was allowed to react with CH<sub>2</sub>FI yielding 76% of the corresponding 1H-1,3-bis(fluoromethyl)-2-methyl imidazolium iodide (**7**) (Scheme 2). Single crystals of **7** were obtained by slow evaporation of a solution of **7** in acetonitrile. The molecular structure of **7** in the crystal is shown in Figure 5.



**Scheme 2.** Synthesis of bisfluoromethyl imidazole **7**.

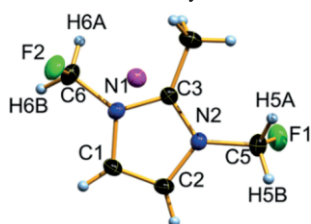


**Figure 5.** Molecular structure of **7** in the crystal. DIAMOND representation, thermal ellipsoids are drawn with 50% probability. Selected bond length and angles of **7**: F1–C5, 1.370(3); C5–N2, 1.439(3); F2–C6, 1.376(3); C6–N1, 1.444(3); F1–C5–N2, 108.8(2); F2–C6–N1, 108.6(2); F1–C5–N2–C3, –92.2(3); F2–C6–N1–C3, –84.5(3).

Both nitrogen atoms in compound **7** display a trigonal planar environment. As compared to **6a** [N2–C5: 1.420(3)  $\text{\AA}$ , 1.423(2)  $\text{\AA}$ ], the N–C bond length in **7** [N2–C5: 1.439(3)  $\text{\AA}$ , N1–C6 (1.444(3)  $\text{\AA}$ )] are slightly longer. However, the C5–F1 and C6–F2 distances of 1.370(3)  $\text{\AA}$  and 1.376(3)  $\text{\AA}$ , respectively, are significantly shorter than in **6a** [1.400(3)  $\text{\AA}$ , 1.388(2)  $\text{\AA}$ ] and are similar to those reported for PCH<sub>2</sub>F [1.379(5)  $\text{\AA}$ ],<sup>[6]</sup> CH<sub>2</sub>FI [1.380(17)  $\text{\AA}$ ],<sup>[21]</sup> or CH<sub>2</sub>FBr [1.377(4)  $\text{\AA}$ ].<sup>[21]</sup> The intermolecular interactions also change dramatically, due to the introduction of ionic charges and of the iodide anion. The H $\cdots$ N close contacts, which are characteristic for **6a**, are replaced by H $\cdots$ I and H $\cdots$ F contacts (Figure 6c, e). As a result, about 62% attractive contacts are present in **7**, in contrast to 42.5% in **6b**. This is in accord with the fact, that **7** can be heated up to 252  $^\circ$ C without observable decomposition. The non-distinct spikes for the H $\cdots$ F and H $\cdots$ I contacts (Figure 6d) and the sum  $d_i + d_e$  ( $d_i$  = distance from the Hirshfeld surface to the nearest atom interior;  $d_e$  = distance from the Hirshfeld surface to the nearest atom exterior) indicate, that these interactions are weak (Table 2).<sup>[17,18]</sup> As an example, the strongest H $\cdots$ I contact (Figure 6h), with a distance of 3.15(2)  $\text{\AA}$  is by far longer than the only weak interaction with a distance of 2.83(2)  $\text{\AA}$  found in [PPh<sub>3</sub>CH<sub>2</sub>F]I.<sup>[6]</sup> A similar weak contact was observed in [PPh<sub>3</sub>CH<sub>2</sub>OH]I, where

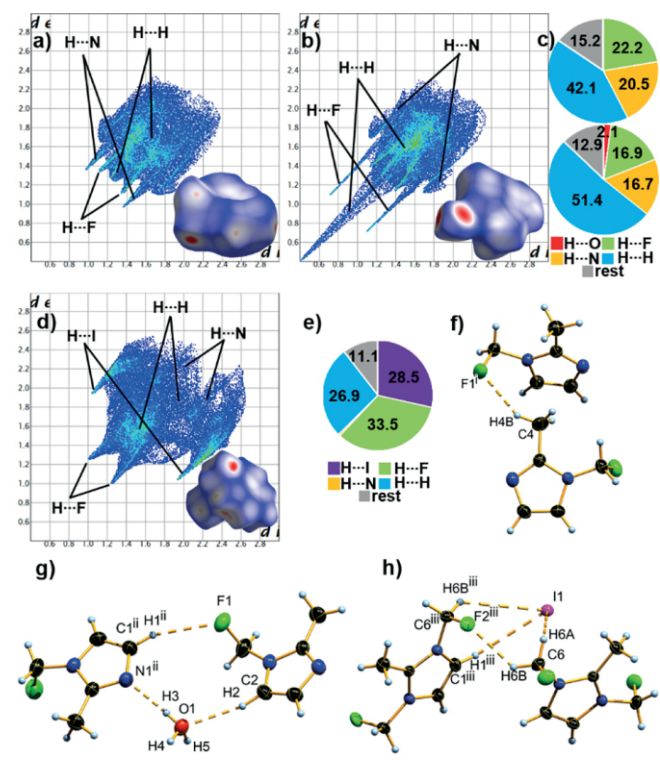


**Figure 6.** Two-dimensional fingerprint plot as well as the corresponding Hirshfeld surface (bottom right in 2D plot) of **6a** (a), **6b** (b) and **7** (d). Color coding: white, distance  $d$  equals VDW distance; blue,  $d$  exceeds VDW distance; red,  $d$  is smaller than VDW distance. Population of close contacts of **6a** (c) top, **6b** (c) bottom and **7** (e) in crystal stacking. Strongest hydrogen bonds in **6a** (f), **6b** (g) and **7** (h). DIAMOND representation. Thermal ellipsoids are drawn at 50% probability level. Symmetry codes: *i*) 0.5+ $x$ , 0.5– $y$ , 1– $z$ ; *ii*) 1– $x$ , 0.5+ $y$ , 0.5– $z$ ; *iii*) 1.5– $x$ , 0.5+ $y$ ,  $z$ .

the CH...I interaction corresponds to a distance of 3.092(2) Å.<sup>[23]</sup> The weak interactions are responsible that **7** decomposes at 252 °C without melting and this occurs by approx. 50 °C lower than the melting point of its methyl analogue (312 °C).<sup>[24]</sup>

## Conclusions

In summary, we have synthesized new fluoromethylated nitrogen containing heterocycles, which can act as interesting and versatile ligands for transition metals. Single crystal X-ray diffraction studies reveal for the first time reliable structural information on CH<sub>2</sub>F bonded to nitrogen. Only weak fluorine hydrogen interactions were observed in the structures of all compounds investigated. However, the intermolecular interactions in the crystal were identified to be responsible for the low melting points of the fluoromethyl derivatives.

Comparing the fluoromethyl- and hydroxymethyl phthalimide, the lower number of strong O...H contacts decreases the melting point of the fluoromethyl derivative. Fluoromethyl imidazole derivatives show almost negligible interactions in the crystal, therefore the melting points of those are low.

**Supporting Information** (see footnote on the first page of this article): contains NMR- and crystallographic data.

## Acknowledgements

Financial support by the Ludwig-Maximilian University is grateful acknowledged. We are thankful to F-Select GmbH for a generous donation of fluoriodomethane. Open access funding enabled and organized by Projekt DEAL.

**Keywords:** Monofluoromethylation; Fluorine effect; Heterocycles; Fluoriodomethane; X-ray diffraction

## References

- [1] L. An, Y.-L. Xiao, Q.-Q. Min, X. Zhang, *Angew. Chem. Int. Ed.* **2015**, *54*, 9079–9083.
- [2] a) K. Makino, H. Yoshioka, Institute of Physical and Chemical Research, JP63179866A, **1988**; b) Y. L. Chen, Pfizer Inc., EP276942A1, **1988**.
- [3] K. Masuda, S. Kida, N. Yoshikawa, M. Katou, T. Kato, M. Nakajima, E. Kojima, M. Yonehara, Shionogi & Co. Ltd., WO2011074560A1, **2011**.
- [4] J. Stehouwer, M. Goodman, C. Kilts, C. Nemeroff, Emory University, WO2010096426A2, **2010**.
- [5] Q.-H. Zheng, M. Gao, B. H. Mock, S. Wang, T. Hara, R. Nazih, M. A. Miller, T. J. Receveur, J. C. Lopshire, W. J. Groh, D. P. Zipes, G. D. Hutchins, T. R. DeGrado, *Bioorg. Med. Chem. Lett.* **2007**, *17*, 2220–2224.
- [6] M. Reichel, J. Martens, E. Woellner, L. Huber, A. Kornath, K. Karaghiosoff, *Eur. J. Inorg. Chem.* **2019**, *2019*, 2530–2534.
- [7] H. Boehme, M. Hilp, *Chem. Ber.* **1970**, *103*, 104–111.
- [8] W. Zhang, L. Zhu, J. Hu, *Tetrahedron* **2007**, *63*, 10569–10575.
- [9] K. G. Grozinger, R. W. Kriwacki, S. F. Leonard, T. P. Pitner, *J. Org. Chem.* **1993**, *58*, 709–713.
- [10] X.-N. Hua, W.-Q. Liao, Y.-Y. Tang, P.-F. Li, P.-P. Shi, D. Zhao, R.-G. Xiong, *J. Am. Chem. Soc.* **2018**, *140*, 12296–12302.
- [11] K. Makino, H. Yoshioka, Institute of Physical and Chemical Research, JP63179866A, **1988**.
- [12] a) M. Rueda-Becerril, C. Chatalova Sazepin, J. C. T. Leung, T. Okbinoglu, P. Kennepohl, J.-F. Paquin, G. M. Sammis, *J. Am. Chem. Soc.* **2012**, *134*, 4026–4029; b) F. Yin, Z. Wang, Z. Li, C. Li, *J. Am. Chem. Soc.* **2012**, *134*, 10401–10404; c) K. Makino, H. Yoshioka, *J. Fluorine Chem.* **1987**, *35*, 677–683; d) R. Senatore, M. Malik, M. Spreitzer, W. Holzer, V. Pace, *Org. Lett.* **2020**, *22*, 1345–1349.
- [13] M. Reichel, J. Martens, C. C. Unger, K. Karaghiosoff, *Phosphorus Sulfur Silicon Relat. Elem.* **2019**, *194*, 467–468.
- [14] F. H. Allen, O. Kennard, D. G. Watson, L. Brammer, A. G. Orpen, R. Taylor, *J. Chem. Soc. Perkin Trans. 2* **1987**, S1–S19.
- [15] Z.-J. Quan, R.-G. Ren, X.-D. Jia, Y.-X. Da, Z. Zhang, X.-C. Wang, *Tetrahedron* **2011**, *67*, 2462–2467.
- [16] K. Zheng, C. Yao, *Shiyu Huagong* **2004**, *33*, 145–148.
- [17] C. Zhang, X. Xue, Y. Cao, Y. Zhou, H. Li, J. Zhou, T. Gao, *CrystEngComm* **2013**, *15*, 6837–6844.
- [18] T. Steiner, *Angew. Chem. Int. Ed.* **2002**, *41*, 48–76.
- [19] G. Laus, A. Schwaerzler, G. Bentivoglio, M. Hummel, V. Kahlenberg, K. Wurst, E. Kristeva, J. Schutz, H. Kopacka, C. Kreutz, G. Bonn, Y. Andriyko, G. Nauer, H. Schottenberger, *Z. Naturforsch. B* **2008**, *63*, 447–464.
- [20] M. Lissel, S. Schmidt, B. Neumann, *Synthesis* **1986**, 382–383.
- [21] M. Feller, K. Lux, A. Kornath, *Eur. J. Inorg. Chem.* **2015**, *2015*, 5357–5362.
- [22] a) H. Tian, Z. Yu, A. Hagfeldt, L. Kloo, L. Sun, *J. Am. Chem. Soc.* **2011**, *133*, 9413–9422; b) J. Sarasin, E. Wegmann, *Helv. Chim. Acta* **1924**, *7*, 720–723.
- [23] M. C. Davis, D. A. Parrish, *Synth. Commun.* **2008**, *38*, 3909–3918.
- [24] A. Fuerstner, M. Alcarazo, R. Goddard, C. W. Lehmann, *Angew. Chem. Int. Ed.* **2008**, *47*, 3210–3214.

Received: June 19, 2020

Published Online: July 29, 2020